CER4 Encodes an Alcohol-Forming Fatty Acyl-Coenzyme A Reductase Involved in Cuticular Wax Production in Arabidopsis[1][W]

Owen Rowland[2], Huanquan Zheng, Shelley R. Hepworth[2], Patricia Lam, Reinhard Jetter, and Ljerka Kunst*

Department of Botany (O.R., H.Z., S.R.H., P.L., R.J., L.K.) and Department of Chemistry (R.J.), University of British Columbia, Vancouver, British Columbia, Canada V6T 1Z1

A waxy cuticle that serves as a protective barrier against uncontrolled water loss and environmental damage coats the aerial surfaces of land plants. It is composed of a cutin polymer matrix and waxes. Cuticular waxes are complex mixtures of very-long-chain fatty acids and their derivatives. We report here the molecular cloning and characterization of *CER4*, a wax biosynthetic gene from Arabidopsis (*Arabidopsis thaliana*). Arabidopsis *cer4* mutants exhibit major decreases in stem primary alcohols and wax esters, and slightly elevated levels of aldehydes, alkanes, secondary alcohols, and ketones. This phenotype suggested that *CER4* encoded an alcohol-forming fatty acyl-coenzyme A reductase (FAR). We identified eight FAR-like genes in Arabidopsis that are highly related to an alcohol-forming FAR expressed in seeds of jojoba (*Simmondsia chinensis*). Molecular characterization of *CER4* alleles and genomic complementation revealed that one of these eight genes, *At4g33790*, encoded the FAR required for cuticular wax production. Expression of *CER4* cDNA in yeast (*Saccharomyces cerevisiae*) resulted in the accumulation of C24:0 and C26:0 primary alcohols. Fully functional green fluorescent protein-tagged CER4 protein was localized to the endoplasmic reticulum in yeast cells by confocal microscopy. Analysis of gene expression by reverse transcription-PCR indicated that *CER4* was expressed in leaves, stems, flowers, siliques, and roots. Expression of a β-glucuronidase reporter gene driven by the *CER4* promoter in transgenic plants was detected in epidermal cells of leaves and stems, consistent with a dedicated role for CER4 in cuticular wax biosynthesis. *CER4* was also expressed in all cell types in the elongation zone of young roots. These data indicate that CER4 is an alcohol-forming FAR that has specificity for very-long-chain fatty acids and is responsible for the synthesis of primary alcohols in the epidermal cells of aerial tissues and in roots.

A continuous lipophilic layer called the cuticle covers most of the aerial surfaces of vascular plants. The cuticle is synthesized by epidermal cells and is one of their distinctive features. The main function of the cuticle is to serve as a waterproof barrier. It restricts nonstomatal water loss and repels rainwater, thus minimizing the deposition of dust, pollen, and spores (Kerstiens, 1996; Riederer and Schreiber, 2001). The cuticle also protects underlying tissues from excess levels of UV radiation, mechanical damage, as well as bacterial and fungal pathogens (Jenks et al., 2002) and insects (Eigenbrode and Espelie, 1995). Furthermore, the cuticle has a critical role in plant development by preventing the fusion of cell walls from adjacent organs (Sieber et al., 2000).

The cuticle consists primarily of cutin and waxes. Cutin, the main structural component of the cuticle, is composed of C16 and C18 hydroxy and epoxy fatty acid monomers (Heredia, 2003) that form a three-dimensional matrix overlaying the epidermal cell wall. Cuticular waxes are both embedded in the cutin matrix (intracuticular) and cover the cuticle proper (epicuticular). Epicuticular waxes are often present in the form of crystals, which if dense enough impart a whitish bloom to plant surfaces.

Cuticular waxes are complex mixtures of lipids, mostly composed of very-long-chain aliphatic molecules, including primary and secondary alcohols, aldehydes, alkanes, ketones, and esters that are derived from saturated very-long-chain fatty acids (VLCFAs). Each lipid class can be present as a series of characteristic chain lengths (e.g. C24, C26, C28, C30) or one chain length may predominate. Wax load and composition varies considerably between different plant species (Post-Beittenmiller, 1996). Even within a plant species, wax composition varies between the different organs and tissues, as well as during development. Wax deposition may also be influenced during organ growth by a variety of environmental signals, such as light, moisture, and temperature (Kolattukudy, 1996).

The first step in wax biosynthesis is the elongation of saturated C16 and C18 fatty acyl-CoAs, produced in the plastid, to generate VLCFA wax precursors between

[1] This work was supported by a grant from the National Sciences and Engineering Research Council of Canada.

[2] Present address: Department of Biology, Carleton University, 1125 Colonel By Drive, Ottawa, Ontario, Canada K1S 5B6.

* Corresponding author; e-mail kunst@interchange.ubc.ca; fax 604–822–6089.

The author responsible for distribution of materials integral to the findings presented in this article in accordance with the policy described in the Instructions for Authors (www.plantphysiol.org) is: Ljerka Kunst (kunst@interchange.ubc.ca).

[W] The online version of this article contains Web-only data.

www.plantphysiol.org/cgi/doi/10.1104/pp.106.086785

20 and 34 carbons in length. Fatty acid elongation is catalyzed by an endoplasmic reticulum (ER)-associated, multienzyme system referred to as the fatty acid elongase (von Wettstein-Knowles, 1982). Once the very-long-chain fatty acyl-CoA chains are synthesized, they are either converted into aldehyde intermediates and then into odd-chain alkanes, secondary alcohols, and ketones via a decarbonylation pathway (Cheesbrough and Kolattukudy, 1984; Schneider-Belhaddad and Kolattukudy, 2000), or into primary alcohols and wax esters via an acyl-reduction pathway (Kunst and Samuels, 2003).

Even though major wax biosynthetic steps have been defined, our knowledge of the enzymes involved and the nature of the biochemical reactions that they catalyze is limited. Only a small number of genes cloned from Arabidopsis (*Arabidopsis thaliana*) and maize (*Zea mays*) encode biosynthetic enzymes of known function. For example, CER6, KCS1, GL8A, GL8B, and CER10 are components of the fatty acid elongases required to generate VLCFA wax precursors (Xu et al., 1997; Millar et al., 1999; Todd et al., 1999; Fiebig et al., 2000; Dietrich et al., 2005; Zheng et al., 2005). CER1, GL1, and WAX2 are proteins that all contain three His-rich motifs characteristic of a class of integral membrane enzymes (Aarts et al., 1995; Hansen et al., 1997; Chen et al., 2003; Kurata et al., 2003; Sturaro et al., 2005). Although this is suggestive of metabolic roles, the biochemical activities associated with these proteins are presently unknown. Other genes have been proposed to encode regulatory proteins involved in wax production: CER2, GL2, CER3, GL15, and WIN1/SHN1 (Tacke et al., 1995; Hannoufa et al., 1996; Moose and Sisco, 1996; Negruk et al., 1996; Xia et al., 1996; Aharoni et al., 2004; Broun et al., 2004), but their regulatory functions remain to be confirmed. Finally, *CER5* encodes a plasma membrane-localized ATP-binding cassette transporter that is required for transport of wax to the cuticle (Pighin and Zheng et al., 2004).

It is notable that, among the wax-related genes cloned thus far, none specify an enzyme that catalyzes a reaction following fatty acid elongation. Therefore, the most detailed information on the acyl-reduction pathway currently comes from early reports on the biochemistry of plant cuticular wax formation and from recent investigations characterizing related genes involved in the formation of VLCFA primary alcohols and alkyl esters in other organisms and tissues. The biochemistry of wax alcohol formation was first examined in *Brassica oleracea* and led to the proposal that this is a two-step process carried out by two separate enzymes, an NADH-dependent fatty acyl reductase (FAR) that reduces the fatty acyl-CoAs to free aldehydes and an NADPH-dependent aldehyde reductase that converts the aldehydes to primary alcohols (Kolattukudy, 1971). Subsequent biochemical studies in jojoba (*Simmondsia chinensis*) embryos (Pollard et al., 1979) and pea (*Pisum sativum*) leaves (Vioque and Kolattukudy, 1997), and functional expression of genes specifying alcohol-forming FARs from jojoba (Metz et al., 2000), silkmoth (*Bombyx mori*; Moto et al., 2003), mouse (*Mus musculus*), and human (*Homo sapiens*) cells (Cheng and Russell, 2004) in heterologous systems revealed that alcohol biosynthesis from VLCFAs can be carried out by a single alcohol-forming FAR without the release of a possible aldehyde intermediate.

For Arabidopsis, corresponding FARs involved in cuticular wax biosynthesis have not been investigated and it is currently unknown whether the acyl-reduction pathway proceeds in one or two enzymatic steps from acyl-CoA precursors to primary alcohols. Earlier studies (Hannoufa et al., 1993; McNevin et al., 1993; Jenks et al., 1995) have established that the stems of Arabidopsis *cer4* mutants almost completely lack primary alcohols (and wax esters), suggesting that *CER4* is involved in the acyl-reduction pathway (Jenks et al., 1995). Two alleles of *cer4* were independently identified by visual screening of mutants that have glossy stem surfaces compared to the glaucous appearance of wild-type Arabidopsis stems. *cer4-1* is a fast neutron-induced mutation in the Landsberg *erecta* (L*er*) ecotype (Koornneef et al., 1989) and *cer4-2* is a T-DNA-induced mutation in the Wassilewskija (Ws) ecotype (McNevin et al., 1993).

The goal of this work was to clone and characterize the gene disrupted in Arabidopsis *cer4* mutants to investigate whether the CER4 protein (1) is indeed a FAR; (2) can form aldehyde and/or primary alcohols; (3) has chain length specificity for very-long-chain fatty acyl substrates; and (4) is responsible for wax alcohol formation in all organs of the plant; and (5) to determine its subcellular location.

RESULTS

Molecular Identification of the *CER4* Gene

A query of the Arabidopsis genome database with the deduced amino acid sequence of the jojoba FAR using BLAST search programs revealed a group of eight sequences in the Arabidopsis genome that were highly related to the jojoba FAR (28%–54% amino acid sequence identity) over their entire length (Fig. 1). One of these sequences is *MS2* (*At3g11980*), the gene that encodes a tapetum-specific protein essential for pollen fertility (Aarts et al., 1997), but the functions of the other seven FAR-like genes in Arabidopsis have not been investigated. To determine whether any of these genes corresponded to *CER4* involved in the formation of primary alcohols in the cuticle, we correlated the positions of identified FAR-like sequences with the position of the *cer4* mutation on the Arabidopsis genetic map. Only one of the putative FARs, *At4g33790*, matched the genetic map position of *CER4* on chromosome 4 at 60.9 cM (Koornneef et al., 1989) and was thus considered a candidate for being *CER4*.

Sequencing of the *At4g33790* genomic clone revealed an error in the deposited genomic sequence (GenBank accession no. NC_003075) through comparisons to

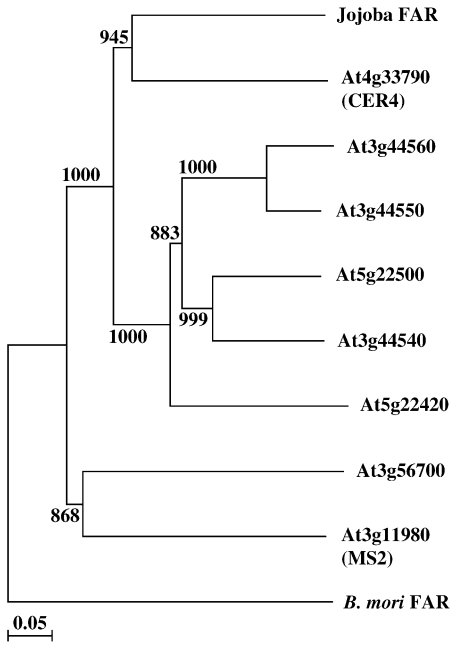

Figure 1. Phylogenetic tree of alcohol-forming FARs from Arabidopsis and jojoba. The coding sequences for the eight Arabidopsis FARs were obtained from annotated gene databases and then, when necessary, manually reannotated to obtain the likely coding sequences. The deduced Arabidopsis polypeptides, the jojoba FAR protein (GenBank accession no. AAD38039), and the more distantly related silkmoth FAR protein (GenBank accession no. AC79425) were aligned using ClustalX 1.83 (Thompson et al., 1997), and a tree was generated using the neighbor-joining method. Silkmoth FAR was used to root the tree. Branch length scale bar = 0.05. Bootstrap values (out of 1,000 replicates) for each cluster are shown at the nodes.

deposited full-length cDNA sequences (GenBank accession nos. AY057657 and AY070065; Yamada et al., 2003). This error was an extra nucleotide causing a frame shift in the predicted coding sequence. The corrected *At4g33790* gene consists of 10 exons (Fig. 2A) and the entire exon-intron region is 3,567 bp in length. The full-length cDNA sequence contains an open reading frame of 1,482 bp encoding a 493-amino acid protein. PCR amplification of the *At4g33790* gene in the *cer4-1* mutant indicated the presence of a deletion and/or rearrangement of at least 3,350 bp spanning 500 bp of the promoter region, the 5′-untranslated region, and at least 2,800 bp downstream of the translation start. A T-DNA insertion is present in the fourth intron of *At4g33790* (at nucleotide 1,960 relative to the start codon) in the *cer4-2* mutant. The finding that two independently isolated mutant lines with the same glossy stem wax phenotype both had changes in the same gene indicated that CER4 is indeed encoded by *At4g33790*.

To confirm the identity of the *CER4* gene, we also obtained two SALK T-DNA insertion lines, SALK_038693 (*cer4-3*) and SALK_000575 (*cer4-4*), containing T-DNA insertions in the fifth exon (nucleotide 2,225) and fourth intron (nucleotide 1,755), respectively, of the *At4g33790* gene from the Arabidopsis Biological Resource Center (ABRC). Homozygotes of *cer4-3* and *cer4-4* exhibited glossy stem phenotypes similar to the previously characterized *cer4-1* and *cer4-2* lines. Finally, the extent of *cer4* gene disruption was examined by semiquantitative reverse transcription (RT)-PCR. Very low levels of *CER4* mRNA were detected in the *cer4-2*, *cer4-3*, and *cer4-4* lines, whereas no transcript was found in *cer4-1* (Fig. 2B). Taken together, these results demonstrate that *CER4* is identical to the FAR-like gene *At4g33790*.

Chemical and Morphological Changes in Stem Cuticular Wax of *cer4* Mutants

The total wax loads on stems of all three wild-type lines of Arabidopsis were found to be very similar under the growth conditions used here, ranging from 20 μg/cm^2 for Ws to 23 μg/cm^2 for L*er* and Columbia-0 (Col-0; Table I). The total wax coverage on inflorescence stems of the four mutant lines did not differ from respective wild types. Furthermore, both the absolute amounts and the relative proportions of the fatty acids, aldehydes, alkanes, secondary alcohols, and ketones did not differ between the wax mixtures of the wild-type lines and between the *cer4* lines and the corresponding wild types (Table I; Fig. 3). The only compound classes affected by CER4 mutations were the primary alcohols and the alkyl esters, reduced from wild-type levels of 2 to 3 μg/cm^2 and 1 to 4 μg/cm^2, respectively, to only trace amounts in the mutant lines (Tables I and II).

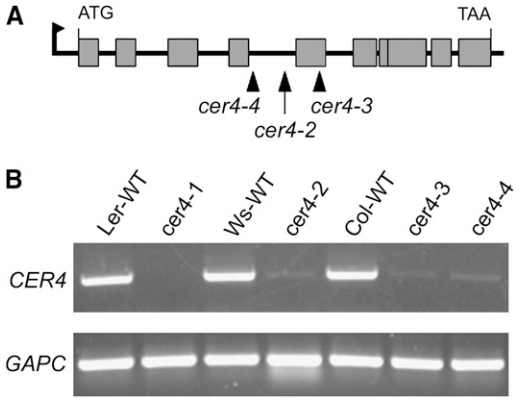

Figure 2. Structure of the *CER4* gene and transcript levels in *cer4* mutant lines. A, Exon-intron structure of the corrected *At4g33790* (*CER4*) gene. Gray boxes represent exons. The *cer4-1* allele has a deletion of the entire *CER4* gene that was caused by fast neutron irradiation. Black triangles represent T-DNA insertion sites present in the other *cer4* alleles characterized. *cer4-2* and *cer4-4* (SALK_000575) carry T-DNA insertions in the fourth intron. *cer4-3* (SALK_038693) carries a T-DNA insertion in the fifth exon. B, Top, Semiquantitative RT-PCR of steady-state *CER4* mRNA in *cer4* mutants compared to the corresponding wild-type ecotypes. RNA was isolated from stem tissue. B, Bottom, Expression of *GAPC* as a loading control for the corresponding lanes in the top image.

Table I. *Composition of cuticular waxes on inflorescence stems of various Arabidopsis cer4 mutant lines and corresponding wild types*

Mean values ($\mu g/cm^2$) of total wax loads and coverage of individual compound classes are given with SDS ($n = 4$).

	Total Load	Fatty Acids	Aldehydes	Alkanes	Secondary Alcohols	Ketones	Primary Alcohols	Not Identified
L*er* (wild type)	22.6 ± 0.7	0.6 ± 0.0	1.1 ± 0.0	8.9 ± 0.3	3.7 ± 0.3	4.4 ± 0.2	2.3 ± 0.2	1.5 ± 0.1
cer4-1	24.8 ± 2.5	0.8 ± 0.1	1.1 ± 0.1	11.0 ± 1.0	4.6 ± 0.4	5.4 ± 0.6	0.1 ± 0.0	1.8 ± 0.3
cer4-1 + At4g33790	24.4 ± 2.3	0.6 ± 0.1	1.3 ± 0.2	7.6 ± 0.7	3.2 ± 0.2	4.2 ± 0.5	6.0 ± 0.5	1.5 ± 0.2
Ws (wild type)	19.9 ± 2.3	0.4 ± 0.0	0.1 ± 0.0	7.6 ± 1.0	2.4 ± 0.4	3.8 ± 0.5	2.6 ± 0.2	1.8 ± 0.3
cer4-2	21.2 ± 0.8	0.5 ± 0.0	1.7 ± 0.1	9.5 ± 0.5	3.0 ± 0.2	4.3 ± 0.4	0.1 ± 0.0	2.0 ± 0.1
Col-0 (wild type)	23.1 ± 0.8	0.5 ± 0.0	2.0 ± 0.1	9.0 ± 0.5	3.8 ± 0.3	3.8 ± 0.1	2.2 ± 0.0	1.7 ± 0.1
cer4-3 (SALK038693)	23.9 ± 2.3	0.4 ± 0.1	2.9 ± 0.2	10.4 ± 1.1	4.7 ± 0.5	3.6 ± 0.4	0.2 ± 0.0	1.8 ± 0.2
cer4-4 (SALK000575)	24.4 ± 1.3	0.5 ± 0.0	2.5 ± 0.2	10.7 ± 0.6	4.4 ± 0.4	4.1 ± 0.3	0.2 ± 0.0	2.0 ± 0.1

A close examination of the chain length patterns within compound classes revealed that most of the individual wax compounds were unchanged in *cer4-1*. The most drastic effect was found for the C24, C26, and C28 primary alcohols, all three compounds being reduced to trace amounts in the stem wax of all four mutant lines. In contrast, C30 primary alcohol still accumulated in the *cer4-1* cuticle, reaching approximately 16% of wild-type levels (Fig. 3). Similar chain length patterns were found for the primary alcohols in *cer4-2* and *cer4-3*, whereas *cer4-4* showed a drastic reduction of C24 and C26 alcohols, and partially reduced amounts of C28 and C30 alcohols (data not shown).

The alkyl esters of the wild-type lines showed chain lengths ranging from C38 to C54, with a strong predominance of even-numbered homologs and a maximum for C44 (Table II). In contrast to this, the mutant lines *cer4-1*, *cer4-2*, and *cer4-3* had largely reduced levels of even-numbered esters, but not of odd-numbered compounds. The remaining even-numbered esters

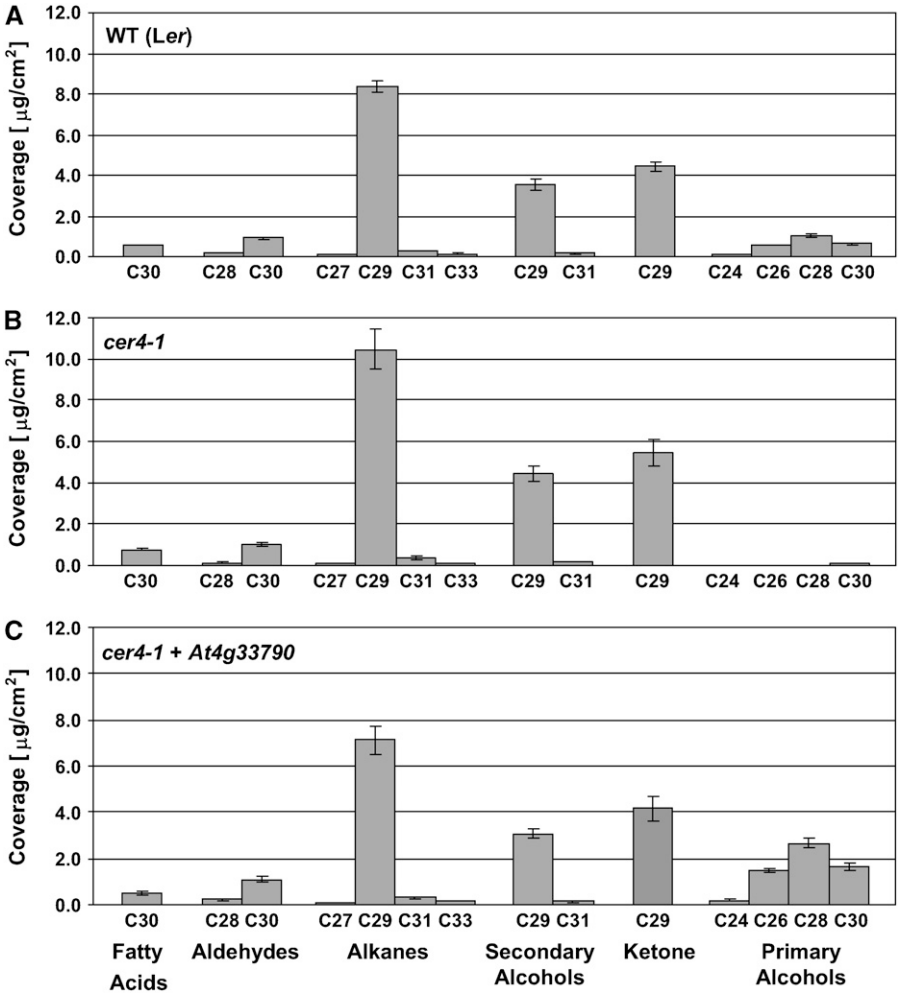

Figure 3. Cuticular wax composition on stems of Arabidopsis plants. A, Wild-type (L*er*). B, *cer4-1* mutant. C, *cer4-1* mutant expressing genomic DNA containing *At4g33790* (molecular complementation of *cer4-1*). Each bar represents the amount of a specific wax constituent, labeled on the *x* axis by a chemical class and a carbon chain length. Each value is the mean of four independent measurements of individual plants. Error bars = SDS.

Table II. *Chain length distribution of wax esters and of alkyl groups constituting these esters*

Relative compositions (%) are given for all four *cer4* mutant lines and Col-0 wild type based on single analyses that were in all cases confirmed in a second entirely independent experiment.

	Wild Type (Col-0)	*cer4-1*	*cer4-2*	*cer4-3*	*cer4-4*
Ester chain length					
38	1.5	2.9	3.1	1.0	0.4
39	0.3	0.8	0.6	0.2	0.2
40	4.2	2.7	2.0	0.7	1.0
41	0.7	1.6	1.3	0.7	0.5
42	21.9	5.7	4.0	1.6	6.6
43	1.2	3.6	4.1	4.0	1.9
44	30.3	11.7	8.1	5.2	15.2
45	2.5	18.8	20.7	25.4	9.0
46	23.1	16.0	11.7	11.2	27.2
47	0.6	6.3	4.9	8.2	3.0
48	9.9	9.3	7.8	4.2	13.6
49	0.1	5.4	5.0	6.9	2.5
50	3.1	8.0	10.5	10.0	10.2
51	0.0	1.2	1.4	2.6	0.9
52	0.6	5.6	8.4	8.7	4.2
53	0.0	0.1	1.1	1.6	0.4
54	0.1	0.3	5.3	7.7	3.3
Alkyl chain length					
22	6.6	19.5	16.1	13.1	5.1
24	8.7	9.1	7.3	3.8	4.7
26	40.8	16.3	20.2	17.1	28.3
28	32.1	24.9	32.7	40.8	35.2
30	10.5	24.3	20.0	21.7	24.6
32	1.3	6.0	3.7	3.4	2.1

showed a bimodal distribution with maxima at C46 and at C50 to C54. The ester fraction was dominated by the C45 ester, which, according to mass spectrometry (MS) data, consisted mainly of C16:0 acid esterified with a C29 alcohol. Because this is the predominant chain length of the secondary alcohols in Arabidopsis stem wax, it seems very likely that this residual ester contains the secondary alcohols nonacosan-14-ol and -15-ol. These alcohols were not further analyzed in the *cer4* mutant esters because secondary alcohols are formed on the decarbonylation pathway without involvement of FAR enzymes and the acyl reduction pathway. The even-numbered alkyl moieties of all the esters were quantified using MS data and summarized according to the alcohol chain lengths present. Whereas Col-0 wild-type esters were dominated by C26 alkyl chains, the mutant lines *cer4-1*, *cer4-2*, and *cer4-3* were characterized by drastically decreased amounts of this alcohol. Instead, they had notably increased levels of C22 and C30 alcohols in their stem wax esters, together with varying levels of C24 and C28 alcohols. The wax of *cer4-4* showed an ester composition intermediate between wild-type and the other three mutant lines.

Even though the total stem wax loads of the *cer4* plants were similar to wild-type plants, the stems of all four mutant lines appeared glossy. This indicated that the epicuticular wax crystals on the *cer4* stems were affected by the mutations. Because these crystals had not been reported for *cer4* plants before, we examined the density and shape of wax crystals on stems of *cer4-1* plants by scanning electron microscopy (SEM; Fig. 4). A dense array of epicuticular wax crystals consisting of vertical rods, tubes, longitudinal bundles of rodlets, and horizontal, reticulate platelets cover the stem surfaces of wild-type Arabidopsis (Fig. 4, A and B). Conversely, the stem surfaces of *cer4-1* plants are almost devoid of wax crystals and instead have a thick film of wax with a relatively smooth surface (Fig. 4, C and D), accounting for the change in surface light reflectance.

Both the wax chemical and the surface micromorphological phenotypes could be rescued by complementation with the *At4g33790* genomic sequence (Fig. 3; Table I), providing further evidence that we have identified the *CER4* gene.

Heterologous Expression of CER4 in Yeast

To verify that CER4 is an alcohol-forming FAR involved in the production of very-long-chain primary alcohols, we expressed the 1,482-bp coding region of the *CER4* gene in Saccharomyces under the control of the yeast (*Saccharomyces cerevisiae*) *GAL1* promoter. Under inducing conditions, cells transformed with an empty-vector control accumulated C16:0, C16:1, C18:0, C18:1, and C26:0 fatty acids, but no fatty alcohols could be detected (Fig. 5A). Conversely, yeast cells expressing CER4 produced two novel compounds. They were identified as primary alcohols C24:0-OH and C26:0-OH (Fig. 5B), based on their gas chromatography (GC) behavior and MS characteristics. The CER4-expressing cells also consistently accumulated greater levels of C26:0 fatty acid compared to the control yeast. No primary alcohols derived from saturated and monounsaturated C16 and C18 fatty acids could be detected.

The subcellular localization of the CER4 FAR was carried out in yeast expressing *CER4* cDNA N-terminally tagged with green fluorescent protein (GFP) under the

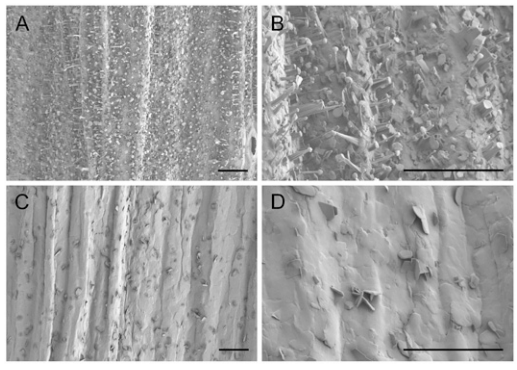

Figure 4. Epicuticular wax crystal formation on Arabidopsis stem surfaces detected by SEM. A and B, Wild type (L*er*) at 1,500× and 5,000× magnification, respectively. C and D, *cer4-1* mutant at 1,500× and 5,000× magnification, respectively. Bars = 10 μm.

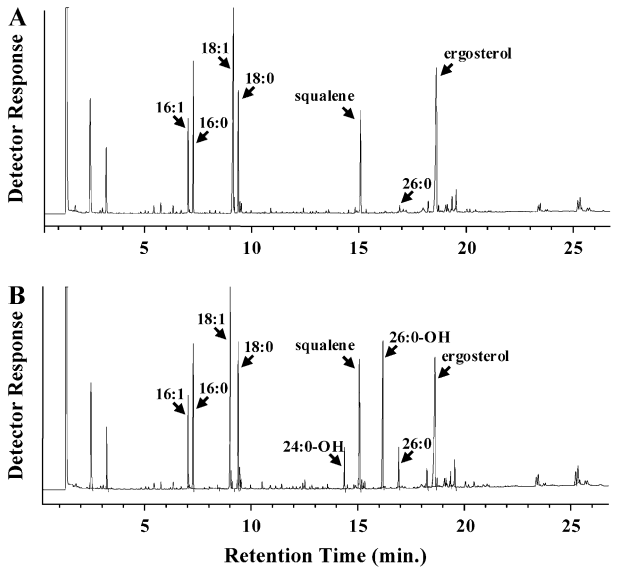

Figure 5. Heterologous expression of *CER4* in yeast. A and B, Gas chromatograms of trimethylsilyl-derivatized lipids that were chloroform extracted from yeast cells hosting the empty-vector control p423-GAL1 (A) or yeast cells expressing *CER4* from the p423-GAL1/CER4 vector (B). Major peaks are identified. The identities of the C24 and C26 primary alcohol peaks were confirmed by GC-MS (data not shown).

control of the *GAL1* promoter. The fusion of the GFP epitope to the CER4 protein did not affect the FAR activity of the modified enzyme in yeast (data not shown) and allowed us to visualize it by confocal microscopy. This experiment revealed a fluorescence pattern typical of the yeast ER (Fig. 6A, arrow). Counterstaining of yeast cells with hexyl rhodamine B, a dye that can stain the ER, outlined the same cellular domains (Fig. 6, C–E), confirming that CER4 resides in the ER in yeast.

Characterization of the Predicted CER4 Protein

The *CER4* transcript encodes a polypeptide of 493 amino acids with an estimated molecular mass of 56.0 kD. The predicted CER4 protein sequence is 54% identical with the NADPH-dependent membrane-associated alcohol-forming FAR from jojoba embryos (Metz et al., 2000) and is identical in length (Fig. 7). CER4 exhibits extensive sequence similarities to Arabidopsis MS2 (36% amino acid identity) and the other six members of the Arabidopsis FAR family (31%–49% amino acid identity; Supplemental Fig. S1). The coding sequences for the uncharacterized Arabidopsis FARs were obtained from annotated gene databases and then, when necessary, manually reannotated to obtain the more likely coding sequences and deduced polypeptide sequences. Five of the Arabidopsis FARs are similar in size to CER4, ranging from 482 to 496 residues in length. At3g56700 and MS2 (At3g11980) have amino-terminal extensions of unknown function and are 548 and 616 residues in length, respectively. CER4 is the Arabidopsis FAR most closely related to the biochemically characterized jojoba FAR (Fig. 1). CER4 is also highly related to the wheat (*Triticum aestivum*) anther-specific protein TAA1a (42% amino acid identity) that has been shown to synthesize primary fatty alcohols thought to be important for pollen formation and function (Wang et al., 2002; Fig. 7). In addition, CER4 shows short regions of amino acid identity to the functionally assessed pheromone gland FAR from silkmoth (Moto et al., 2003) and two mouse enzymes, FAR1 and FAR2 (Cheng and Russell, 2004; Fig. 7).

The jojoba FAR is thought to be an integral membrane protein containing two membrane-spanning domains between residues 309 to 329 and between residues 378 to 398. CER4 has a similar number of hydrophobic residues in these two predicted segments (Fig. 7). However, hydropathy plots and other sequence analysis programs do not reveal strong transmembrane domains anywhere in the CER4 protein sequence. It thus remains uncertain whether these segments are true transmembrane regions in the FAR enzymes. The deduced CER4 amino acid sequence also lacks the typical NAD(P)H binding motif or Rossmann fold: GXGXX(G/A) (Wierenga et al., 1986). Aarts et al. (1997) speculated that MS2 binds NAD(P)H through a related nucleotide-binding sequence (I/V/F)X(I/L/V) TGXTGFL(G/A) and CER4 contains this motif between residues 19 and 29 (Fig. 7).

Analysis of *CER4* Gene Expression

Semiquantitative RT-PCR was used to investigate the transcription profile of the *CER4* gene in various whole tissues (Fig. 8). Aerial tissue samples were derived from 6-week-old Arabidopsis plants and the root tissue sample from 14-d-old seedlings. *CER4* was expressed in all tissues, but to varying levels. Highest transcript accumulation was detected in open flowers and roots. Modest transcript levels were observed in stems, closed flowers, and siliques; low, but consistently

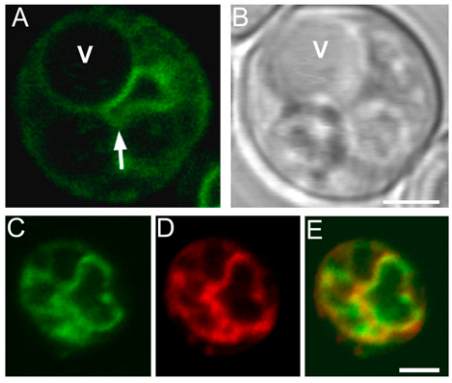

Figure 6. Subcellular localization of CER4 in yeast. A, GFP fluorescence of yeast cells expressing GFP-CER4. The arrow identifies the ER localization of GFP-CER4. The vacuole of the cell is identified by a V. B, Bright-field image of the yeast cell depicted in A. C to E, Colocalization of GFP-CER4 labeled on the ER (C) and the ER membrane stained by hexyl rhodamine B (D), with the merged images shown in E. Bars = 1 μm.

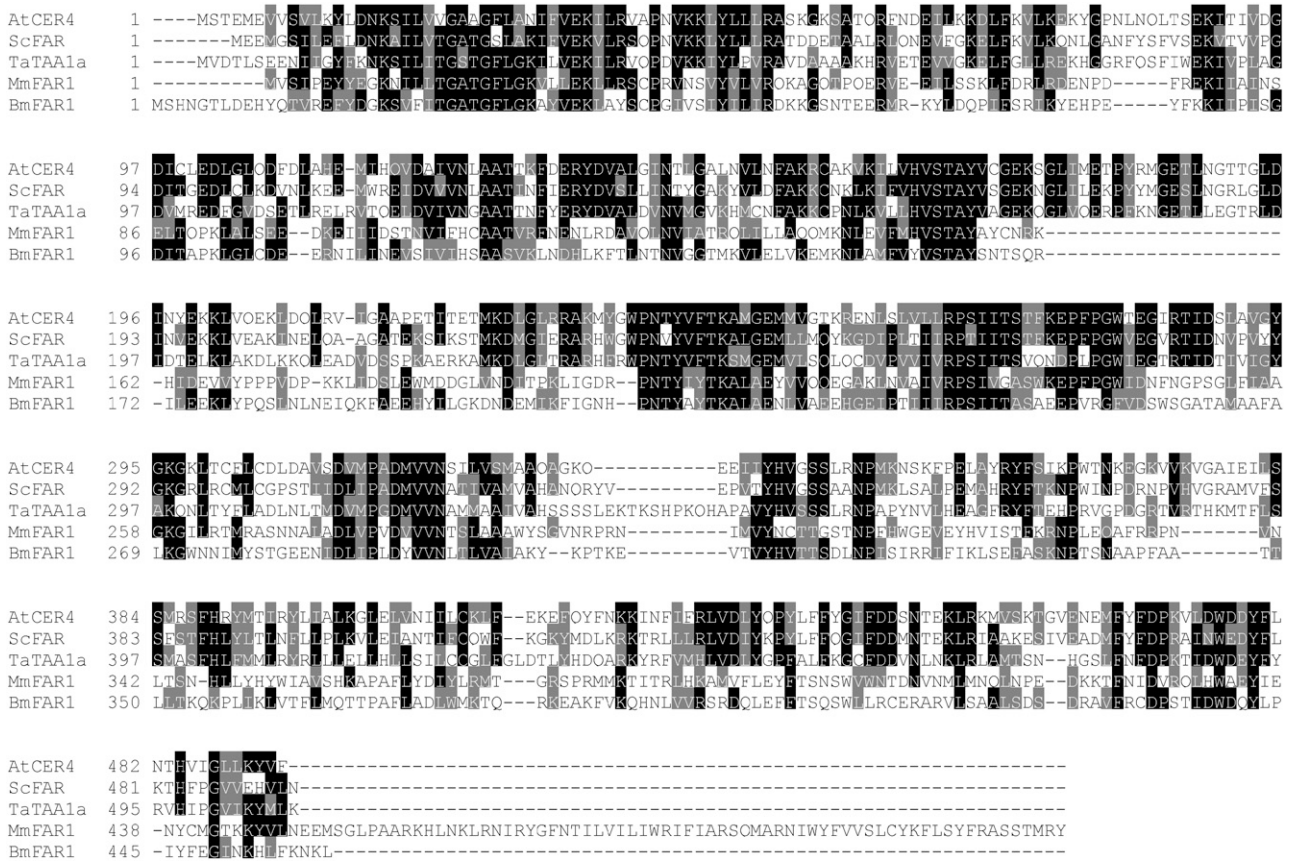

Figure 7. Sequence alignment of alcohol-forming FARs from various species. GenBank accession numbers of the sequences used are: Arabidopsis AtCER4, AAL49822; jojoba ScFAR, AC79425; wheat TaTAA1a, CAD30692; mouse MmFAR1, AAH07178; and silkmoth BmFAR, AAD38039. Identical residues are highlighted on a black background; similar amino acids are shown on a gray background.

detectable, *CER4* transcripts were observed in rosette and cauline leaves.

To analyze the cell-type expression pattern of *CER4* in detail, the 2.1 kb of genomic sequence immediately upstream of the *CER4* coding region was fused to the *β*-glucuronidase (GUS) reporter gene (CER4pro:GUS) and the construct was used to transform Arabidopsis. Tissue samples from 20 independent transgenic lines were stained for GUS activity, with four of these lines being characterized in detail. Consistent with RT-PCR analysis, reporter gene expression was observed in both shoots and roots (Fig. 9). In the stem, *CER4* was expressed along the entire length exclusively in the epidermal cells (Fig. 9, A and B). We confirmed the epidermis-specific expression of *CER4* in the inflorescence by in situ hybridization (Fig. 9C) and observed that *CER4* expression was confined to the region below the shoot apical and floral meristems.

In rosette leaves, CER4pro:GUS was strongly expressed in the trichomes, which are specialized epidermal cells (Fig. 9E). This very restricted expression pattern in leaves may explain the low levels of the *CER4* transcript present in whole-leaf tissues because the transcript would be diluted by the surrounding pavement cells and underlying mesophyll cells. Expression of *CER4* in cauline leaves was more widespread, being detected in trichomes, pavement cells, and the vasculature, and was especially high at the base of the leaf (Fig. 9D). However, this was not reflected by higher levels of total expression detected by RT-PCR using whole-tissue samples from cauline leaves (Fig. 8).

In flowers, CER4pro-directed GUS activity was detected in the petals, the filaments of the stamens, and the carpel (Fig. 9F). In situ hybridization of the *CER4*

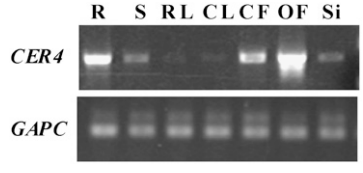

Figure 8. Expression of *CER4* in different tissues of wild-type Arabidopsis (Col-0). Top, Semiquantitative RT-PCR of steady-state *CER4* mRNA using total RNA prepared from roots (R), stems (S), rosette leaves (RL), cauline leaves (CL), closed flowers (CF), opened flowers (OF), and siliques (Si). Bottom, Expression of *GAPC* as a loading control for the corresponding lanes in the top image.

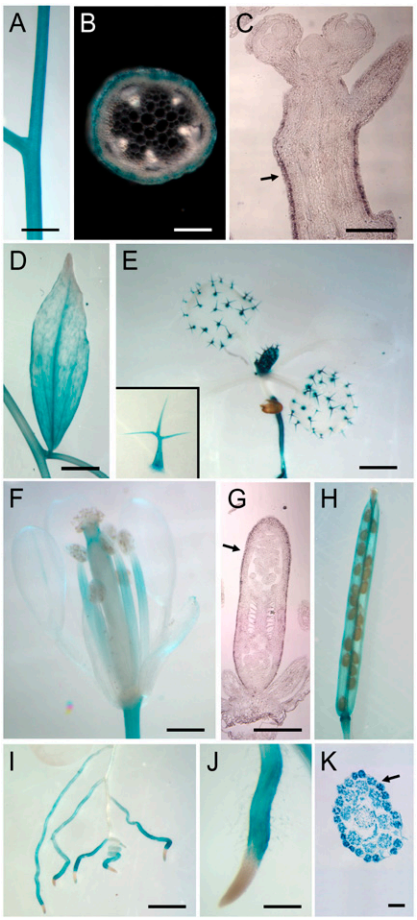

Figure 9. Expression patterns of *CER4* detected in *CER4* promoter:GUS lines and by in situ localization. A, B, D to F, and H to K, Stained tissues expressing the *CER4* promoter:GUS reporter gene: whole stems (A); stem cross-section (B); cauline leaf (D); seedling with trichome in inset (E); flower (F); silique (H); whole root (I); root tip (J); and root cross-section (K). C and G, Expression of *CER4* as detected by in situ hybridization: inflorescence apex (C) and carpel (G).

transcript verified the expression in the carpel and showed that this expression was epidermis specific (Fig. 9G). In siliques, CER4pro:GUS activity was present throughout the outer layer of the silique, but no activity was observed in the seeds (Fig. 9H).

Unexpectedly, we also detected *CER4* expression in the central and lateral roots of 14-d-old seedlings (Fig. 9I), but not in the root tip (Fig. 9J). *CER4* expression was strongest in the elongation zone behind the root tip and appeared to diminish in the older sections of the differentiation zone (Fig. 9I). In the elongation zone, GUS activity was detected in all cell types (Fig. 9K), although GUS staining appeared more pronounced in the epidermal cells compared to interior cell types.

DISCUSSION

Primary alcohols account for 10% to 15% of the total wax load on wild-type Arabidopsis stems and 15% to 25% on Arabidopsis leaves either as free alcohols or in the form of wax esters. Mutations in *CER4* virtually abolish the formation of primary alcohols in both plant organs, indicating that CER4 is the key enzyme catalyzing their biosynthesis. In this study, we have used the *cer4* mutants to clone the *CER4* (*At4g33790*) gene and characterize the functions of CER4 in wax production.

The *CER4* (*At4g33790*) gene encodes a protein with an estimated molecular mass of 56 kD, similar to values reported for the jojoba and pea FAR enzymes (Vioque and Kolattukudy, 1997; Metz et al., 2000), and has extensive sequence similarity to the jojoba protein. FAR enzymes catalyze the cleavage of the thioester bond of the fatty acyl-CoA substrate and the reduction of the resulting fatty acid to a primary alcohol by transfer of electrons from an NAD(P)H cofactor. To directly assess the reductase activity of the CER4 FAR and to investigate its substrate specificity, we expressed the *CER4* cDNA in yeast. *CER4*-expressing yeast accumulated free very-long-chain alcohols of characteristic C24 and C26 length. Wild-type yeast cells also make C20 and C22 fatty acids for the synthesis of sphingolipids. However, C20 and C22 free alcohols were not detected in the *CER4* expressors, indicating that these acyl groups are either not substrates for the CER4 FAR or not accessible to the CER4 enzyme. The absence of shorter alcohols, especially the C16 and C18 ones, suggests that CER4 is unable to use the abundant endogenous saturated and monounsaturated C16 and C18 acyl-CoA as substrates. This is in contrast to a FAR from silkmoth, which produced C16 and C18 fatty alcohols when heterologously expressed in yeast (Moto et al., 2003), and the FAR from jojoba, which produced C16:0 and C18:1 fatty alcohols when expressed in bacteria (Metz et al., 2000). Yeast transformants expressing the CER4 FAR failed to produce wax esters, indicating that CER4 has no capacity to form wax esters from the generated primary alcohols, at least in yeast cells.

The CER4 substrate specificity revealed in yeast is in good agreement with the established wax profiles of *cer4* mutants, which lack C24 to C28 free alcohols as reported here and previously (Hannoufa et al., 1993; McNevin et al., 1993; Jenks et al., 1995). However, *cer4* mutants still accumulate significant amounts of C30 alcohol, suggesting that an additional FAR isozyme is likely involved in its production. With the exception of MS2, a tapetum-specific protein essential for pollen development (Aarts et al., 1997), the functions of the other six Arabidopsis FAR isozymes are unknown. Microarray analysis indicates that expression of five of these genes is limited to specific tissue types (stems, roots, flowers, or seeds), whereas one is widely expressed (Schmid et al., 2005). Of these, only *At3g56700* appeared to be highly expressed in stems and is thus a candidate for generating the remaining C30 primary alcohol. As expected, the alkyl ester composition in *cer4* mutants is significantly affected due to the lack of C24 to C28 primary alcohols that can be used by the putative wax synthase to generate the cuticular alkyl esters.

Interestingly, despite the massive reduction in primary alcohol and alkyl ester levels, *cer4* mutants have almost wild-type stem wax loads (Table I) and yet their stems are strongly glossy. The SEM survey of the *cer4* stem surface showed that they are covered with a relatively smooth film and are virtually devoid of wax crystals, resulting in a glossy stem appearance. These data indicate that primary alcohols and/or wax esters are required for epicuticular wax crystal formation. It is unlikely, however, that the wax crystals themselves are formed from these two wax components alone because alkanes, secondary alcohols, and ketones make up the majority of the Arabidopsis stem wax load (approximately 75%) and are expected to make the major contribution to crystal form. It thus remains unclear how the lack of acyl-reduction products prevents wax crystal formation.

The *CER4* transcript was detected exclusively in the epidermal cells of stems. Expression of *CER4* in the epidermal layer of the shoot was anticipated based on the phenotype of *cer4* mutants, which lack primary alcohols in cuticular wax deposited on the stem surface. This suggests that the primary function of CER4 is in cuticular wax formation, at least in stems. *CER4* was also expressed in the epidermal cells of leaves, but was confined to trichome cell types in rosette leaves. This trichome-specific pattern of expression has been observed for *CER2* (Xia et al., 1997) and for *WAX2/YRE1* (Kurata et al., 2003). We analyzed the leaf wax composition of four trichomeless mutants—*gl1*, *gl2*, *gl3*, and *ttg1*—and surprisingly failed to detect a reduction in primary alcohol levels (data not shown). Additional work is required to determine whether *CER4* gene expression is altered in these mutants or whether a low level of *CER4* expression in the pavement cells of wild-type plants accounts for the primary alcohol production in rosette leaves. It is also possible that *CER4* is expressed to higher levels earlier in leaf development than that examined here. In the latter case, the primary alcohols would be formed very early in leaf development. The highest level of expression of *CER4* was found in the elongation zone of the root, where the transcript was present in all cell types. Our root expression data are in good agreement with the digital in situ information available for Arabidopsis roots (Birnbaum et al., 2003), which also localized the highest *CER4* expression signals in the epidermis, stele, and endodermis of the elongation and differentiation zones. Transcripts of several other cuticle-related genes have also been detected in the root tissue, namely, *FDH* (Yephremov et al., 1999; Pruitt et al., 2000), *LCR* (Wellesen et al., 2001), *WAX2/YRE* (Kurata et al., 2003), *LACS2* (Schnurr et al., 2004), *ACE/HTH* (Krolikowski et al., 2003; Kurdyukov et al., 2006a), *CER5* (Pighin and Zheng et al., 2004), and BDG (Kurdyukov et al., 2006b), suggesting that a protective lipid layer similar to the cuticle is deposited in the cell walls of root cells.

Examination of the active GFP-tagged CER4 in yeast by confocal microscopy revealed that this FAR resides in the ER. ER localization of an alcohol-forming FAR was already suggested for the jojoba embryo enzyme, which was membrane bound and associated with the ER membrane fraction (Metz et al., 2000). It is likely that CER4 is located in the ER in planta, although our attempts to express functional GFP-tagged versions of CER4 in Arabidopsis have thus far been unsuccessful and alternative methods of localization are ongoing. CER4 FAR is the first wax biosynthetic enzyme subsequent of fatty acid elongation for which subcellular location has been determined. The fatty elongase components CER6, a condensing enzyme, and CER10, an enoyl-CoA reductase, have also been localized to the ER using GFP fusions (Kunst and Samuels, 2003; Zheng et al., 2005). The question remains whether the final step of the acyl-reduction pathway, production of alkyl esters from free fatty acids and primary alcohols, is also confined to the ER or whether the alkyl esters are formed in another cellular compartment. Similarly, the enzymes of the decarbonylation pathway have not been positively identified and so the location of this pathway needs to be determined. The nature of the ER membrane association of CER4 also needs to be further investigated in the future. Transmembrane prediction programs failed to detect classical membrane-spanning domains in CER4 and the transmembrane domains proposed for other FARs are not strong and are not generally conserved (Metz et al., 2000; Wang et al., 2002; O. Rowland, unpublished data). It is possible that CER4, and perhaps other FARs, are associated with the membrane through other means, such as a posttranslationally attached lipid.

In summary, we have cloned the *CER4* gene disrupted in the *cer4* wax-deficient mutants of Arabidopsis and demonstrate that it encodes an ER-localized FAR. CER4 is specifically involved in the production of C24 to C28 very-long-chain primary alcohols, one of the major cuticular wax components found on Arabidopsis shoots.

MATERIALS AND METHODS

Plant Material and Growth Conditions

SALK T-DNA insertional lines, SALK_038693 and SALK_000575 (Col-0 ecotype), and *cer4-1* (L*er* ecotype) mutant seeds were obtained from the ABRC (www.arabidopsis.org). *cer4-2* (Ws ecotype) was a gift from Dr. Bertrand Lemieux (York University). Seeds were stratified for 3 to 4 d at 4°C, and were then germinated on AT-agar plates (Somerville and Ogren, 1982) at 20°C under continuous light (100 μE m^{-2} s^{-1} of photosynthetically active radiation). Ten-day-old seedlings were transplanted to soil (Sunshine Mix 5; SunGro) and grown at 22°C under long-day conditions (16-h-light/8-h-dark cycle).

Wax Extraction and Analysis

Wax load was determined on 6-week-old Arabidopsis (*Arabidopsis thaliana*) plants. Stems, leaves, and siliques were immersed in chloroform for 30 s to remove epi- and intracuticular waxes. After extraction, wax samples were evaporated to dryness under a stream of nitrogen, dissolved in 50 μL of *N*, *O*-bis(trimethylsilyl) trifluoroacetamide (BSTFA) with 1% trimethylchlorosilane (TMCS; Pierce), and derivatized at 80°C for 90 min. Samples were then analyzed by gas-liquid chromatography as described in Pighin et al. (2004). Quantification of compounds was based on flame ionization detector peak

areas, which were converted to mass units by comparison with an internal standard, 17:1 methylester, which was added to each sample tube prior to extraction.

For wax ester analyses, stem cuticular wax mixtures of Arabidopsis wild-type and *cer4* mutant lines were separated by thin-layer chromatography on silica gel using 1,1,1-trichloroethane as the mobile phase. Compound classes were localized by staining with primuline and UV light, removed from the plates, eluted with $CHCl_3$, filtered, concentrated in a stream of N_2, and stored at 4°C. The fraction containing alkyl esters (R_f 0.13) was subjected to detailed GC analyses. A GC-flame ionization detector was employed to quantify the relative amounts of ester homologs, whereas GC-MS was used to determine the isomer composition for each ester chain length based on acyl fragments $RCOOH_2^+$.

SEM

Segments from the apical 1 cm of the stem were mounted onto SEM stubs, allowed to dry, and then coated with gold particles in a SEMPrep2 sputter coater (Nanotech). The coated samples were viewed with a Hitachi S4700 field emission SEM using an accelerating voltage of 1 kV and a working distance of 12 mm.

Protein Alignment and Phylogenetic Analysis

Protein sequences were aligned with the ClustalW 1.83 program (Thompson et al., 1997) using default parameters (http://www.ebi.ac.uk/clustalw). Pretty printing of the alignments was done using BOXSHADE 3.21 (http://www.ch.embnet.org/software/BOX_form.html). For construction of the phylogenetic tree, the proteins were first aligned with the ClustalX 1.83 program using the BLOSUM series matrix and default parameters (http://bips.u-strasbg.fr/fr/Documentation/ClustalX). The phylogenetic tree was generated by the neighbor-joining method using the njplot program available with the ClustalX 1.83 program.

Molecular Complementation of *cer4* Phenotype

A 6,138-bp DNA fragment containing the coding region of *At4g33790* was amplified by PCR from genomic DNA isolated from wild-type L*er* plants. This fragment contained 2,160 bp of sequence 5′ of the ATG start codon and 438 bp of sequence 3′ of the stop codon. The primers used for amplification were At4g33790-Prom*Eco*RI (5′-GAGGAATTCTTTCCTTGTAGCCGCCTTTA-3′) and At4g33790-Term*Xba*I (5′-GAGTCTAGAAACTTTACATGGGGGCAATG-3′). To minimize PCR-induced errors, amplification was carried out using the Expand high-fidelity PCR system (Roche Diagnostics). The amplified DNA fragment was digested with *Eco*RI and *Xba*I and cloned into the corresponding sites of pRD400 (Datla et al., 1992). The resulting pRD400/At4g33790 construct was transformed into *Agrobacterium tumefaciens* strain GV3101(pMP90) by electroporation. Transformation of *cer4-1* Arabidopsis plants was performed using the floral-dip method (Clough and Bent, 1998) and transformants were selected on AT-agar plates containing 30 μg mL^{-1} kanamycin (w/v).

Expression and Subcellular Localization of *CER4* in Yeast

We first isolated full-length *CER4* cDNA for expression in yeast (*Saccharomyces cerevisiae*). Total RNA was extracted from wild-type Col-0 plants using TRIzol Reagent (Invitrogen) according to manufacturer's protocol. First-strand cDNA synthesis was carried out using 1 μg of total RNA, oligo$(dT)_{18}$, and SuperScript II reverse transcriptase (Invitrogen). To amplify *CER4* cDNA, PCR was performed using the Expand high-fidelity PCR system (Roche) with 1 μL of cDNA. Primers used for amplification were CER4-F5*Bam*HI (5′-GAGGGATCCATGTCGACAGAAATGGAGGTC-3′) and CER4-R7*Sac*I (5′-CACGAGCTCTTAGAAGACATACTTAAGCAGC-3′). The amplified DNA fragment was digested with *Bam*HI and *Sac*I and cloned into the corresponding sites of pBluescript II SK^+ to generate pBS/CER4. Sequencing of an individual clone confirmed that there were no errors in the *CER4* cDNA. pBS/CER4 was digested with *Eco*RI and *Ecl*136II and cloned between the *Eco*RI and *Eco*RV restriction sites of the yeast expression vector p423-GAL1 (Mumberg et al., 1994) to yield p423-GAL1/CER4.

p423-GAL1/CER4 and an empty-vector p423-GAL1 (control) were transformed into yeast strain W3031A (*MAT*a *ade2-1 his3-11,15 leu2-3,112 trp1-1 ura3-1 can1-100*) according to Gietz and Woods (2002) and grown on minimal medium agar plates lacking His. Individual yeast transformants were then transferred to selective medium agar plates containing 2% (w/v) Gal to induce expression of *CER4*. These plates were incubated at 30°C for 6 d prior to extraction of lipids. For extraction of total lipids, yeast cells were scraped from plates into 1 mL of methanol. After 5 min, 2 mL of chloroform was added and the mixture vortexed. After another 5 min, 0.75 mL of 0.9% (w/v) NaCl was added. Following phase separation, the chloroform phase was transferred to a fresh tube. The samples were evaporated to dryness under a stream of nitrogen and then derivatized with BSTFA plus 1% TMCS and analyzed by gas-liquid chromatography as described above for plant wax analysis.

To generate GFP fused in frame with the coding region of *CER4*, pBS/CER4 was digested with *Bam*HI and *Sac*I and subcloned into the corresponding sites of the binary vector pVKH18-GFPN (Zheng et al., 2005), resulting in pVKH18-GFP-CER4. For expression of GFP-CER4 in yeast, the coding region of GFP-CER4 in pVKH18-GFP-CER4 was released as a *Xba*I-*Ecl*136II fragment and then subcloned between *Spe*I and *Eco*RV of the yeast expression vector p423-GAL1 (Mumberg et al., 1994), yielding p423-GAL1:GFP-CER4. This plasmid was transformed in yeast strain W3031A and GFP-CER4 expression induced as described above for CER4 alone. For subcellular localization, GFP and hexyl rhodamine B fluorescence were examined by confocal microscopy as described by Zheng et al. (2005). The yeast cells were immersed in hexyl rhodamine B solution (1.6 μM) for 30 min prior to analysis.

Semiquantitative RT-PCR Analysis

Aerial tissues used for RNA extractions were harvested from 6-week-old Arabidopsis plants. Whole-root tissue was harvested from 14-d-old seedlings grown on AT-agar plates under continuous light conditions. With the exception of silique tissue, total RNA was extracted using a guanidine-HCl and phenol-chloroform extraction procedure (Logemann et al., 1987). RNA was isolated from siliques using an acid phenol-LiCl extraction procedure (Downing et al., 1992), with the addition of 3 M sodium acetate, pH 5.2, wash at the end to remove excess polysaccharides.

For analysis of the transcription profile of *CER4* by RT-PCR, RNA was reverse transcribed using 1 μg of total RNA template, oligo$(dT)_{18}$, and SuperScript II reverse transcriptase (Invitrogen). One microliter of a 1:1 diluted RT reaction was used as template in a 20-μL reaction with gene-specific primers CER4-F5*Bam*HI (above) and CER4-R3*Eco*RI (5′-CACGAATTCCCCTCAGTCCAACCAGGAAA-3′) designed to amplify a 851-bp cDNA fragment of *CER4*. To examine the extent of gene disruption in each of four *cer4* alleles, gene-specific primers TSH450 (5′-CTTCTTCTGTGATCTTGATGC-3′) and TSH451 (5′-TAGAAGACATACTTAAGCAGCC-3′) that can amplify a 578-bp cDNA fragment of *CER4* were used. The glyceraldehyde-3-P dehydrogenase (*GAPC*) constitutive control was amplified using primers GAPC-p1 (5′-TCAGACTCGAGAAAGCTGCTAC-3′) and GAPC-p2 (5′-GATCAAGTCGACCACACGG-3′), which amplifies a 245-bp cDNA fragment.

CER4 Promoter:GUS Fusion and GUS Histochemical Assay

A DNA fragment containing 2,147 bp of sequence immediately upstream of the ATG start codon of *CER4* was amplified by PCR from Arabidopsis bacterial artificial chromosome T16L1 (AL031394) using the Expand high-fidelity system (Roche Diagnostics). The primers used for amplification were CER4-PROM*Sal*Ifor (5′-GAGGTCGACTTTCCTTGTAGCCGCCTTTA-3′) and CER4-PROM*Xba*Irev (5′-GAGTCTAGAGTATATACGTTTGAGTGAGAGA-3′). The amplified product was digested with *Sal*I and *Xba*I and cloned between the corresponding sites of pBluescript II SK+ to generate pBS/CER4pro. Sequencing of an individual clone confirmed that there were no errors in the *CER4* promoter. pBS/CER4pro was digested with *Sal*I and *Xba*I and cloned between the corresponding sites of pBI101 (CLONTECH) to generate a transcriptional fusion of the CER4 promoter with the GUS reporter gene. This construct was introduced into wild-type Col-0 plants by Agrobacterium-mediated transformation as described above.

GUS staining solution was composed of 50 mM sodium phosphate, pH 7.0, 0.5 mM potassium ferricyanide, 0.5 mM potassium ferrocyanide, 0.1% (v/v) Triton X-100, and 0.5 mg/mL 5-bromo-4-chloro-3-indolyl-β-D-glucuronide (X-Gluc). Aerial tissues were preincubated in heptane for 5 min to remove the cuticle and then vacuum infiltrated with GUS staining solution. Tissues were incubated in GUS staining solution at 37°C for 1 h (root tissue) or 6 h (aerial tissues). For whole tissues, samples were cleared in 70% (v/v) ethanol following staining and visualized using a dissecting light microscope. For

tissue sectioning, GUS-stained tissues were first rinsed for 2 min in 100 mM sodium phosphate buffer, pH 7.0, and then fixed in 2.5% glutaraldehyde in the same phosphate buffer for 12 h at 4°C. Following fixation, samples were rinsed for 2 min in phosphate buffer and dehydrated in 30%, 50%, 70%, 80%, 90%, and three changes of 100% ethanol for 10 min at each concentration. Dehydrated samples were then slowly infiltrated with Spurr's resin. The Spurr's resin was allowed to polymerize for 8 h at 70°C. Ten-micrometer-thick sections from the embedded tissue were cut on a Reichert Om U3 (Reichert-Jung) ultramicrotome and visualized using a light microscope.

In Situ Hybridization

In situ hybridization of Arabidopsis inflorescences (tissue fixation, sectioning, hybridization, signal detection, and probe synthesis) was carried out as described previously (Samach et al., 1997). To synthesize probes, 1,461-bp DNA templates were amplified by PCR from *CER4* cDNA using primers incorporating the T7 RNA polymerase-binding site. For the antisense probe, the primers used were 5′-CGACAGAAATGGAGGTCGTT-3′ and 5′-GATAATACGACTCACTATAGGGCAGCCCAATAACATGTGTG-3′. Sections were photographed using bright-field optics.

Supplemental Data

The following materials are available in the online version of this article.

Supplemental Figure S1. Sequence alignment of alcohol-forming FARs from Arabidopsis.

ACKNOWLEDGMENTS

We thank the ABRC at Ohio State University for the *cer4-1* mutant, Bertrand Lemieux for providing the *cer4-2* mutant, and the Salk Institute for Genomic Analysis Laboratory for providing sequence-indexed Arabidopsis T-DNA insertion mutants *cer4-3* (SALK_038693) and *cer4-4* (SALK_000575). We thank Helena Friesen for the p423GAL1 vector. We are grateful to the Bioimaging Facility at the University of British Columbia for providing microscopy support.

Received July 15, 2006; accepted September 1, 2006; published September 15, 2006.

LITERATURE CITED

Aarts MG, Hodge R, Kalantidis K, Florack D, Wilson ZA, Mulligan BJ, Stiekema WJ, Scott R, Pereira A (1997) The Arabidopsis MALE STERILITY 2 protein shares similarity with reductases in elongation/condensation complexes. Plant J **12:** 615–623

Aarts MGM, Keijzer CJ, Stiekema WJ, Pereira A (1995) Molecular characterization of the CER1 gene of Arabidopsis involved in epicuticular wax biosynthesis and pollen fertility. Plant Cell **7:** 2115–2127

Aharoni A, Dixit S, Jetter R, Thoenes E, van Arkel G, Pereira A (2004) The SHINE clade of AP2 domain transcription factors activates wax biosynthesis, alters cuticle properties, and confers drought tolerance when overexpressed in Arabidopsis. Plant Cell **16:** 2463–2480

Birnbaum K, Shasha DE, Wang JY, Jung JW, Lambert GM, Galbraith DW, Benfey PN (2003) A gene expression map of the Arabidopsis root. Science **302:** 1956–1960

Broun P, Poindexter P, Osborne E, Jiang C-Z, Riechmann JL (2004) WIN1, a transcriptional activator of epidermal wax accumulation in *Arabidopsis*. Proc Natl Acad Sci USA **101:** 4706–4711

Cheesbrough TM, Kolattukudy PE (1984) Alkane biosynthesis by decarbonylation of aldehydes catalyzed by a particulate preparation from *Pisum sativum*. Proc Natl Acad Sci USA **81:** 6613–6617

Chen X, Goodwin SM, Boroff VL, Liu X, Jenks MA (2003) Cloning and characterization of the *WAX2* gene of Arabidopsis involved in cuticle membrane and wax production. Plant Cell **15:** 1170–1185

Cheng JB, Russell DW (2004) Mammalian wax biosynthesis. I. Identification of two fatty acyl-Coenzyme A reductases with different substrate specificities and tissue distributions. J Biol Chem **279:** 37789–37797

Clough SJ, Bent AF (1998) Floral dip: a simplified method for Agrobacterium-mediated transformation of *Arabidopsis thaliana*. Plant J **16:** 735–743

Datla RS, Hammerlindl JK, Panchuk B, Pelcher LE, Keller W (1992) Modified binary plant transformation vectors with the wild-type gene encoding NPTII. Gene **122:** 383–384

Dietrich CR, Perera MA, D Yandeau-Nelson M, Meeley RB, Nikolau BJ, Schnable PS (2005) Characterization of two *GL8* paralogs reveals that the 3-ketoacyl reductase component of fatty acid elongase is essential for maize (*Zea mays L.*) development. Plant J **42:** 844–861

Downing WL, Mauxion F, Fauvarque MO, Reviron MP, de Vienne D, Vartanian N, Giraudat J (1992) A *Brassica napus* transcript encoding a protein related to the Kunitz protease inhibitor family accumulates upon water stress in leaves, not in seeds. Plant J **2:** 685–693

Eigenbrode SD, Espelie KE (1995) Effects of plant epicuticular lipids on insect herbivores. Annu Rev Entomol **40:** 171–194

Fiebig A, Mayfield JA, Miley NL, Chau S, Fischer RL, Preuss D (2000) Alterations in *CER6*, a gene identical to *CUT1*, differentially affect long-chain lipid content on the surface of pollen and stems. Plant Cell **12:** 2001–2008

Gietz RD, Woods RA (2002) Transformation of yeast by the lithium acetate/single-stranded carrier DNA/polyethylene glycol method. Methods Enzymol **350:** 87–96

Hannoufa A, McNevin J, Lemieux B (1993) Epicuticular waxes of *eceriferum* mutants of *Arabidopsis thaliana*. Phytochemistry **33:** 851–855

Hannoufa A, Negruk V, Eisner G, Lemieux B (1996) The *CER3* gene of *Arabidopsis thaliana* is expressed in leaves, stems, roots, flowers and apical meristems. Plant J **10:** 459–467

Hansen JD, Pyee J, Xia Y, Wen TJ, Robertson DS, Kolattukudy PE, Nikolau BJ, Schnable PS (1997) The *glossy1* locus of maize and an epidermis-specific cDNA from *Kleinia odora* define a class of receptor-like proteins required for the normal accumulation of cuticular waxes. Plant Physiol **113:** 1091–1100

Heredia A (2003) Biophysical and biochemical characteristics of cutin, a plant barrier biopolymer. Biochim Biophys Acta **1620:** 1–7

Jenks MA, Eigenbrode SD, Lemieux B (2002) Cuticular waxes of Arabidopsis. *In* CR Somerville, EM Meyerowitz, eds, The Arabidopsis Book. American Society of Plant Biologists, Rockville, MD

Jenks MA, Tuttle HA, Eigenbrode SD, Feldmann KA (1995) Leaf epicuticular waxes of the *eceriferum* mutants in Arabidopsis. Plant Physiol **108:** 369–377

Kerstiens G (1996) Signalling across the divide: a wider perspective of cuticular structure-function relationships. Trends Plant Sci **1:** 125–129

Kolattukudy PE (1971) Enzymatic synthesis of fatty alcohols in *Brassica oleracea*. Arch Biochem Biophys **142:** 701–709

Kolattukudy PE (1996) Biosynthetic pathways of cutin and waxes, their sensitivity to environmental stresses. *In* G Kersteins, ed, Plant Cuticles, An Integrated Functional Approach. BIOS Scientific Publishers, Oxford, pp 83–108

Koornneef M, Hanhart CJ, Thiel F (1989) A genetic and phenotypic description of *eceriferum* (*cer*) mutants in *Arabidopsis thaliana*. J Hered **80:** 118–122

Krolikowski KA, Victor JL, Wagler TN, Lolle SJ, Pruitt RE (2003) Isolation and characterization of the Arabidopsis organ fusion gene HOTHEAD. Plant J **35:** 501–511

Kunst L, Samuels AL (2003) Biosynthesis and secretion of plant cuticular wax. Prog Lipid Res **42:** 51–80

Kurata T, Kawabata-Awai C, Sakuradani E, Shimizu S, Okada K, Wada T (2003) The *YORE-YORE* gene regulates multiple aspects of epidermal cell differentiation in *Arabidopsis*. Plant J **36:** 55–66

Kurdyukov S, Faust A, Nawrath C, Bar S, Voisin D, Efremova N, Franke R, Schreiber L, Saedler H, Metraux JP, et al (2006a) The epidermis-specific extracellular BODYGUARD controls cuticle development and morphogenesis in Arabidopsis. Plant Cell **18:** 321–339

Kurdyukov S, Faust A, Trenkamp S, Bar S, Franke R, Efremova N, Tietjen K, Schreiber L, Saedler H, Yephremov A (2006b) Genetic and biochemical evidence for involvement of HOTHEAD in the biosynthesis of long-chain alpha-,omega-dicarboxylic fatty acids and formation of extracellular matrix. Planta **224:** 315–329

Logemann J, Schell J, Willmitzer L (1987) Improved method for the isolation of RNA from plant tissues. Anal Biochem **163:** 16–20

McNevin JP, Woodward W, Hannoufa A, Feldmann K, Lemieux B (1993) Isolation and characterization of *eceriferum* (*cer*) mutants induced by T-DNA insertions in *Arabidopsis thaliana*. Genome **36:** 610–618

Metz JG, Pollard MR, Anderson L, Hayes TR, Lassner MW (2000) Purification of a jojoba embryo fatty acyl-Coenzyme A reductase and expression of its cDNA in high erucic acid rapeseed. Plant Physiol **122:** 635–644

Millar AA, Clemens S, Zachgo S, Giblin EM, Taylor DC, Kunst L (1999) CUT1, an Arabidopsis gene required for cuticular wax biosynthesis and pollen fertility, encodes a very-long-chain fatty acid condensing enzyme. Plant Cell **11:** 825–838

Moose SP, Sisco PH (1996) *Glossy15*, an *APETALA2*-like gene from maize that regulates leaf epidermal cell identity. Genes Dev **10:** 3018–3027

Moto K, Yoshiga T, Yamamoto M, Takahashi S, Okano K, Ando T, Nakata T, Matsumoto S (2003) Pheromone gland-specific fatty-acyl reductase of the silkmoth, *Bombyx mori*. Proc Natl Acad Sci USA **100:** 9156–9161

Mumberg D, Muller R, Funk M (1994) Regulatable promoters of *Saccharomyces cerevisiae*: comparison of transcriptional activity and their use for heterologous expression. Nucleic Acids Res **22:** 5767–5768

Negruk V, Yang P, Subramanian M, McNevin JP, Lemieux B (1996) Molecular cloning and characterization of the *CER2* gene of *Arabidopsis thaliana*. Plant J **9:** 137–145

Pighin JA, Zheng H, Balakshin LJ, Goodman IP, Western TL, Jetter R, Kunst L, Samuels AL (2004) Plant cuticular lipid export requires an ABC transporter. Science **306:** 702–704

Pollard MR, McKeon T, Gupta LM, Stumpf PK (1979) Studies on biosynthesis of waxes by developing jojoba seed. II. The demonstration of wax biosynthesis by cell-free homogenates. Lipids **14:** 651–662

Post-Beittenmiller D (1996) Biochemistry and molecular biology of wax production in plants. Annu Rev Plant Physiol Plant Mol Biol **47:** 405–430

Pruitt RE, Vielle-Calzada JP, Ploense SE, Grossniklaus U, Lolle SJ (2000) *FIDDLEHEAD*, a gene required to suppress epidermal cell interactions in Arabidopsis, encodes a putative lipid biosynthetic enzyme. Proc Natl Acad Sci USA **97:** 1311–1316

Riederer M, Schreiber L (2001) Protecting against water loss: analysis of the barrier properties of plant cuticles. J Exp Bot **52:** 2023–2032

Samach A, Kohalmi SE, Motte P, Datla R, Haughn GW (1997) Divergence of function and regulation of class B floral organ identity genes. Plant Cell **9:** 559–570

Schmid M, Davison TS, Henz SR, Pape UJ, Demar M, Vingron M, Scholkopf B, Weigel D, Lohmann JU (2005) A gene expression map of *Arabidopsis thaliana* development. Nat Genet **37:** 501–506

Schneider-Belhaddad F, Kolattukudy PE (2000) Solubilization, partial purification and characterization of a fatty aldehyde decarbonylase from a higher plant, *Pisum sativum*. Arch Biochem Biophys **377:** 341–349

Schnurr J, Shockey J, Browse J (2004) The acyl-CoA synthetase encoded by *LACS2* is essential for normal cuticle development in Arabidopsis. Plant Cell **16:** 629–642

Sieber P, Schorderet M, Ryser U, Buchala A, Kolattukudy P, Metraux JP, Nawrath C (2000) Transgenic Arabidopsis plants expressing a fungal cutinase show alterations in the structure and properties of the cuticle and postgenital organ fusions. Plant Cell **12:** 721–738

Somerville CR, Ogren WL (1982) Isolation of photorespiratory mutants of *Arabidopsis*. *In* RB Hallick, NH Chua, eds, Methods in Chloroplast Molecular Biology. Elsevier, New York, pp 129–139

Sturaro M, Hartings H, Schmelzer E, Velasco R, Salamini F, Motto M (2005) Cloning and characterization of *GLOSSY1*, a maize gene involved in cuticle membrane and wax production. Plant Physiol **138:** 478–489

Tacke E, Korfhage C, Michel D, Maddaloni M, Motto M, Lanzini S, Salamini F, Doring HP (1995) Transposon tagging of the maize Glossy2 locus with the transposable element En/Spm. Plant J **8:** 907–917

Thompson JD, Gibson TJ, Plewniak F, Jeanmougin F, Higgins DG (1997) The CLUSTAL_X windows interface: flexible strategies for multiple sequence alignment aided by quality analysis tools. Nucleic Acids Res **25:** 4876–4882

Todd J, Post-Beitenmiller D, Jaworski JG (1999) *KCS1* encodes a fatty acid elongase 3-ketoacyl-CoA synthase affecting wax biosynthesis in *Arabidopsis thaliana*. Plant J **17:** 119–130

Vioque J, Kolattukudy PE (1997) Resolution and purification of an aldehyde-generating and an alcohol-generating fatty acyl-CoA reductase from pea leaves (*Pisum sativum* L.). Arch Biochem Biophys **340:** 64–72

von Wettstein-Knowles PM (1982) Elongase and epicuticular wax biosynthesis. Physiol Veg **20:** 797–809

Wang A, Xia Q, Xie W, Dumonceaux T, Zou J, Datla R, Selvaraj G (2002) Male gametophyte development in bread wheat (*Triticum aestivum* L.): molecular, cellular, and biochemical analyses of a sporophytic contribution to pollen wall ontogeny. Plant J **30:** 613–623

Wellesen K, Durst F, Pinot F, Benveniste I, Nettesheim K, Wisman E, Steiner-Lange S, Saedler H, Yephremov A (2001) Functional analysis of the *LACERATA* gene of Arabidopsis provides evidence for different roles of fatty acid omega-hydroxylation in development. Proc Natl Acad Sci USA **98:** 9694–9699

Wierenga RK, Terpstra P, Hol WG (1986) Prediction of the occurrence of the ADP-binding beta alpha beta-fold in proteins, using an amino acid sequence fingerprint. J Mol Biol **187:** 101–107

Xia YJ, Nicolau BJ, Schnable PS (1996) Cloning and characterization of *CER2*, an Arabidopsis gene that affects cuticular wax accumulation. Plant Cell **8:** 1291–1304

Xia YJ, Nicolau BJ, Schnable PS (1997) Developmental and hormonal regulation of the Arabidopsis *CER2* gene that codes for a nuclear-localized protein required for the normal accumulation of cuticular waxes. Plant Physiol **115:** 925–937

Xu XJ, Dietrich CR, Delledonne M, Xia YJ, Wen TJ, Robertson DS, Nikolau BJ, Schnable PS (1997) Sequence analysis of the cloned *glossy8* gene of maize suggests that it may code for a β-ketoacyl reductase required for the biosynthesis of cuticular waxes. Plant Physiol **115:** 501–510

Yamada K, Lim J, Dale JM, Chen H, Shinn P, Palm CJ, Southwick AM, Wu HC, Kim C, Nguyen M, et al (2003) Empirical analysis of transcriptional activity in the Arabidopsis genome. Science **302:** 842–846

Yephremov A, Wisman E, Huijser P, Huijser C, Wellesen K, Saedler H (1999) Characterization of the *FIDDLEHEAD* gene of Arabidopsis reveals a link between adhesion response and cell differentiation in the epidermis. Plant Cell **11:** 2187–2201

Zheng H, Rowland O, Kunst L (2005) Disruptions of the Arabidopsis enoyl-CoA reductase gene reveal an essential role for very-long-chain fatty acid synthesis in cell expansion during plant morphogenesis. Plant Cell **17:** 1467–1481